Polarizability effect in strong-field ionization: Quenching of the low-energy structure in C_{60}

Yu Hang Lai,[1,*] Cosmin I. Blaga,[1] Junliang Xu,[1] Harald Fuest,[2] Philipp Rupp,[2] Matthias F. Kling,[2,3] Pierre Agostini,[1] and Louis F. DiMauro[1]

[1]*Department of Physics, The Ohio State University, Columbus, Ohio 43210, USA*

[2]*Physics Department, Ludwig-Maximilians-Universität München, D-85748 Garching, Germany*

[3]*Max Planck Institute of Quantum Optics, D-85748 Garching, Germany*

(Received 28 September 2018; published 26 December 2018)

The low-energy photoelectron spectra from strong-field ionization of C_{60} fullerenes and noble gases (xenon and krypton) with 3 μm laser pulses are measured and compared. It is found that the low-energy structure (LES), a universal spikelike feature in the strong-field limit of atoms and small molecules, is significantly suppressed in the C_{60} photoelectron distribution. We propose that the large polarizability of the C_{60} core disrupts the corresponding electron trajectories. In particular, the induced dipole force repels the electron, which opposes the focusing and bunching due to the Coulomb potential that is responsible for the LES, thus leading to its reduction.

DOI: 10.1103/PhysRevA.98.063427

I. INTRODUCTION

The low-energy structure (LES) in strong-field ionization by midinfrared (MIR) laser fields is a spikelike feature appearing in the low-energy portion (a few eV) of photoelectron distributions along the laser polarization [1,2]. In the strong-field limit, i.e., $U_p > I_p$, the LES is observed in rare-gas atoms and diatomic molecules, where U_p and I_p are the ponderomotive and binding energies, respectively. Classical-trajectory simulations have revealed that the LES's result from the Coulomb interaction between the "freed" electron with small drift momentum and its parent ion in the process of multiple forward scattering (also called the "soft-recollision") [3–7]. In particular, if the electron trajectories revisit the parent ion with a very small momentum, then its trajectory is susceptible to the ionic Coulomb potential. As a result, these low-energy trajectories are influenced by the potential, which gives rise to a spectral bunching of electron momentum distribution at the LES position.

Previous theory and experiment suggested that the LES is a universal feature that is not significantly affected by the atomic or molecular structure of the core since the long-range $1/r$ Coulomb potential responsible for the process is target-independent. However, for targets with a large polarizability, the non-Coulombic induced dipole field of the ion might not be negligible compared with the Coulomb field and could possibly alter the electron trajectory under certain circumstances. For example, a recent experiment [8] showed unexpected characteristic in the photoelectron spectrum of naphthalene molecules (polarizability $\alpha \sim 16.5$ Å^3) irradiated by elliptically polarized 0.8 μm pulses, attributed to the induced dipole field. Nonetheless, the majority of targets in the previous studies [1,2,9–14] had small polarizabilities ($\alpha < 10$ Å^3) and so this effect was negligible.

C_{60} fullerene has an exceptionally large polarizability ($\alpha \sim 79$ Å^3), which makes it an attractive system to explore the effect of the induced dipole field, as discussed in [15,16]. The interaction of C_{60} with intense laser fields has been the subject of numerous investigations [17–29] (for a review, please see, e.g., [30,31]) but most of them were restricted to Ti:sapphire wavelengths and not conducted in the strong-field limit. Bhardwaj *et al.* [15,16] reported on the ionization and fragmentation yields as a function of laser intensity at longer wavelengths (<2 μm), but no photoelectron spectrum was recorded. Recently, we have measured the photoelectron energy spectrum of C_{60} irradiated by intense MIR (3 and 3.6 μm) pulses [32] in which the high-energy rescattering plateau was used to retrieve the molecular structure employing laser-induced electron diffraction (LIED) [33–35]. The results implied that in the MIR regime, the dynamics of photoelectrons is well described using the three-step semiclassical model [36,37] within a single-active-electron-like picture [38,39]. Therefore, the theory of the LES, which was developed for atoms, should also be applicable for C_{60}.

Here we investigate the LES in C_{60} ionized by intense 3 μm laser pulses. By comparing the spectrum with the ones from noble gases (Xe and Kr) under the same laser conditions, we find that the LES from C_{60} is significantly weaker than for noble gases. This difference can be attributed to the different polarizability of the species. We also perform classical-trajectory simulations including a polarization term, and we study its effect on the LES structure.

II. EXPERIMENT

The linearly polarized MIR laser pulses were generated using a home-built potassium titanyl arsenate optical parametric amplifier pumped by a 12 mJ, 80 fs, 0.8 μm Ti:sapphire laser system at 1 kHz repetition rate (Spectra Physics: Spitfire Ace). The photoelectron energy spectra were measured using a time-of-flight spectrometer operating in a field-free electron

*lai.244@osu.edu

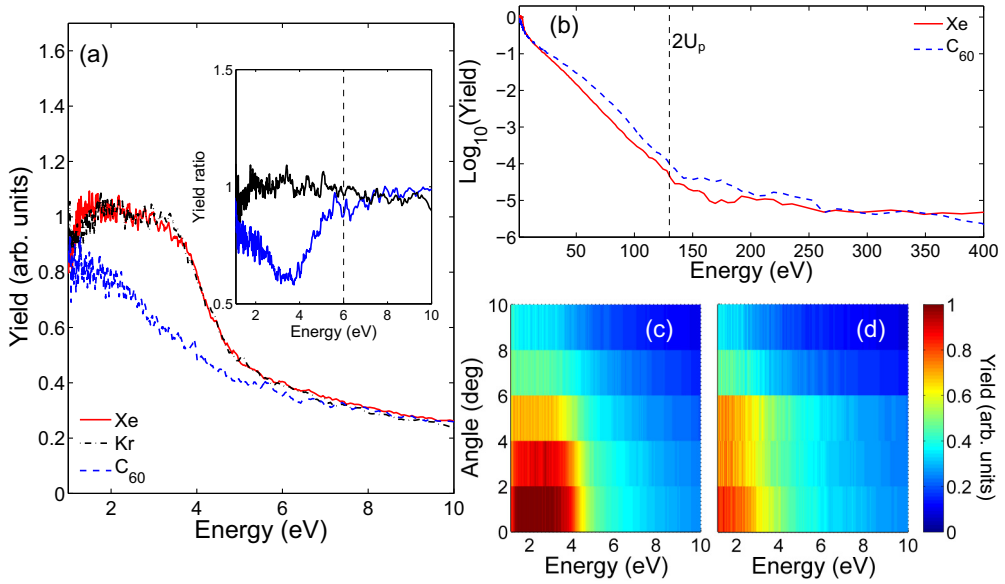

FIG. 1. Comparison of the LES in noble gases and C_{60} ($I = 75$ TW/cm^2, $\lambda = 3$ μm). (a) Low-energy region of the distributions emitted along the laser polarization from Xe (red solid line), Kr (black dashed-dotted line), and C_{60} (blue dashed line). Inset: electron yield ratio between C_{60} and Xe (the blue lower line) and the ratio between Kr and Xe (the black upper line) as a function of energy. (b) Spectra of Xe and C_{60} in (a) but including the high-energy region. The $2U_p$ cutoff of both spectra is at about 140 eV. (c),(d) Photoelectron distributions vs the emission angle with respect to the laser polarization for Xe and C_{60}, respectively. The emission is highly anisotropic for both targets. The angular resolution is 2°.

detection mode with an angular acceptance of 2.1°. The base pressure of the ultrahigh-vacuum chamber is $\sim 10^{-9}$ torr. The C_{60} sample was sublimated from an effusive oven operated at ~600 °C. The laser intensity was calibrated utilizing the $2U_p$ cutoff in the photoelectron spectrum of Xe atoms.

III. RESULTS AND DISCUSSION

Figure 1(a) displays the photoelectron energy spectra emitted along the laser polarization from C_{60} and two noble gases (Xe and Kr) at 3 μm, and the intensity is kept at 75 TW/cm^2. As expected, the LESs in both Xe and Kr, which has an LES cutoff at ~6 eV, are pronounced and identical. Figure 1(b) shows the spectra of Xe and C_{60} in (a) but including both regions of direct and rescattered electrons. Both of them exhibit a characteristic $2U_p$ cutoff at the same energy as indicated by the dashed line. However, the electron yield in the LES region of C_{60} is significantly less abundant. To illustrate the difference of the LES in different species, the electron yield ratios (C_{60}/Xe and Kr/Xe) as a function of energy are shown in the inset of Fig. 1(a). Note that the ratio values themselves do not imply absolute comparisons between the two targets since the yields were in arbitrary units, but the variation in the ratio as a function of energy indicates the relative difference at different energies. While the ratio between Kr and Xe is flat in the LES region as well as in higher energies, the ratio between C_{60} and Xe shows a clear minimum in the LES region. Also, we quantified the "strength" of the LES in each target by the ratio of the yield in the LES region to the yield at higher energies. In Table I, ratios of the yield integrated from 1 to 6 eV to the yield integrated from 6 to 10 eV for the three species are tabulated. The ratio, as a measure of the LES, is about 30% lower for C_{60} than for Xe or Kr.

Another key feature of the LES is that it is highly peaked along the laser polarization direction [9] (only a few degrees) due to the Coulomb focusing mechanism [2]. As shown in Figs. 1(c) and 1(d), the populations of low-energy electrons in both Xe and C_{60} are concentrated at small angles, although the signal from C_{60} is significantly weaker. In fact, the highly anisotropic emission from C_{60} also indicates that thermoelectron emission [40] is not significant in our case. Thus, it is reasonable to attempt a theoretical investigation within the framework of the strong-field ionization with the semiclassical rescattering model.

To investigate the origin of the suppression of the LES in C_{60}, we calculated photoelectron distributions using classical trajectory Monte Carlo simulations, which is known to reproduce the LES [3]. In brief, the electronic wave packet produced by tunnel ionization is mimicked by an ensemble of classical particles whose initial conditions (birth time t_0 and initial transverse momentum p_0) are distributed according to the ADK formula [41]. The subsequent electron motion is modeled classically under the total potential (in atomic units)

$$V(\mathbf{r}, t) = \mathbf{r} \cdot \mathbf{F} - \frac{1}{r} - \frac{\alpha \mathbf{F}(t) \cdot \mathbf{r}}{r^3}, \tag{1}$$

TABLE I. Ratio of the yield integrated from 1 to 6 eV to the yield integrated from 6 to 10 eV for the three species. The error reflects the statistics of the total count in each energy range.

	Ratio
Kr	3.23 ± 0.02
Xe	3.10 ± 0.01
C_{60}	2.37 ± 0.02

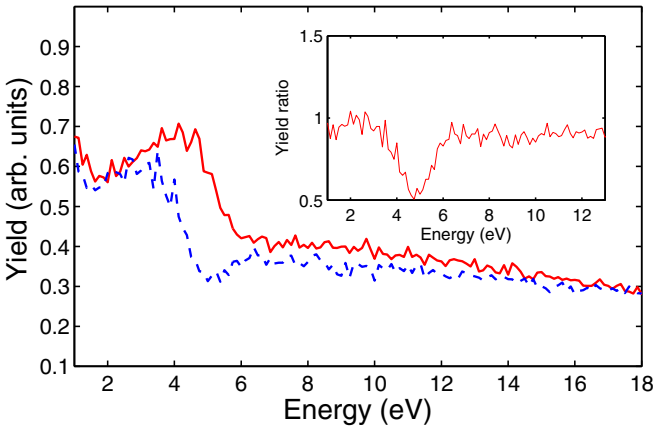

FIG. 2. Photoelectron spectra calculated from classical trajectory simulations with focal averaging with the potential in Eq. (1) with (blue dashed line) and without the induced dipole potential (red solid line); the ratio as a function of energy is in the inset. Parameters in the calculations: $I = 75$ TW/cm^2, $\lambda = 3$ μm; $\alpha = 79$ Å^3.

where $\mathbf{F}(t)$ is the laser field, $-1/r$ is the Coulomb potential, and $-\alpha\mathbf{F}(t)\cdot\mathbf{r}/r^3$ is the induced dipole potential where α is the polarizability. Figure 2 shows a comparison between two calculated photoelectron spectra. The blue dashed line shows the calculation with the total potential of Eq. (1), and the red solid line is the result without the induced dipole potential. Clearly, the LES is partially suppressed by the influence of the induced dipole field. The inset of Fig. 2 shows the yield ratio between the two spectra as a function of energy. The suppression of the LES gives rise to the dip between 3 and 6 eV. The agreement between the classical simulation and the experiment is only qualitative, probably because it ignores quantum effects (see, for example, [42]).

According to the simulations, the suppression occurs because the induced dipole force deflects low-energy trajectories away from the LES spectral region, as qualitatively illustrated in Fig. 3. Figure 3(a) recalls the origin of the LES by showing a typical trajectory returning to the core, first at $t \sim 0.75T$ and then later at $t \sim 1.5T$, the second time with a very small momentum (and hence contributing to the low-energy part of the spectrum). By comparison [Fig. 3(b)], a trajectory with a different initial phase returns to $x = 0$ only once. The corresponding transverse component of the Coulomb force, giving rise to the Coulomb focusing effect, is shown by the red dashed lines in Figs. 3(c) and 3(d), respectively. The blue lines in these two panels show the transverse component of the induced dipole force, as discussed in the next paragraph. The key ingredient for the formation of the LES is the Coulomb force acting on the electron upon the soft recollision of the second return, shown by the spike of the red dashed line at $t \sim 1.5T$ [Fig. 3(c)] [3,4,6,7]. This interaction clearly cannot occur for the higher-energy trajectory in Fig. 3(b) because it does not have a second return. Note that the Coulomb interactions at the origin and the first return, indicated by the spikes of the red dashed line at $t \sim 0$ and $t \sim 0.75T$ in Figs. 3(c) and 3(d), also significantly affect the electron trajectories, but they are not the cause of the LES since they do not exclusively affect the low-energy trajectories.

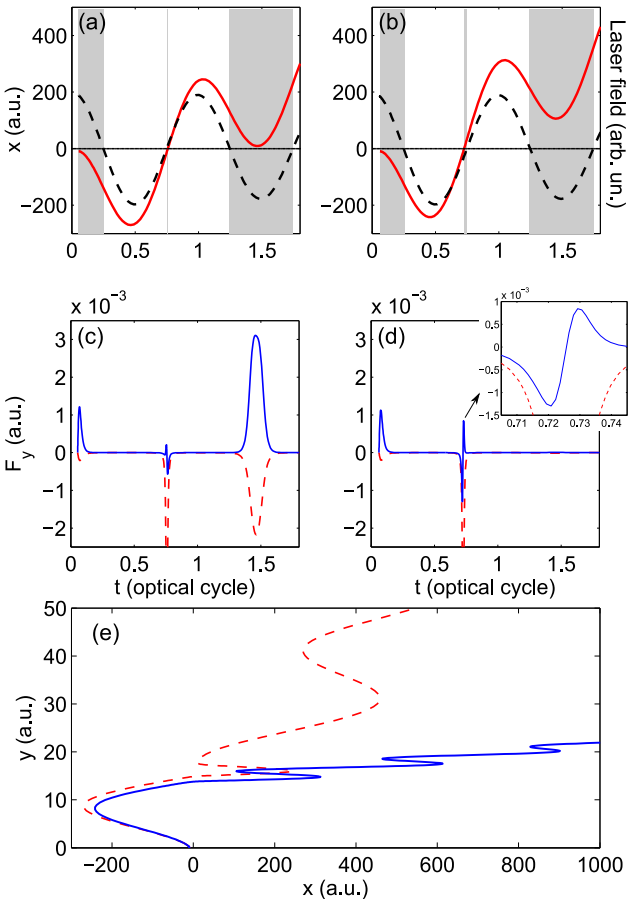

FIG. 3. Sample trajectories. (a) Typical trajectory (red solid line) contributing to the LES (zero momentum at recollision). Initial transverse momentum $p_{y0} = 0.04$ a.u.; ionization phase $\omega t_0 = 0.34$. The black dashed line shows the laser field amplitude. (b) Typical trajectory not contributing to the LES (no recollision). Initial transverse momentum $p_{y0} = 0.04$ a.u.; ionization phase $\omega t_0 = 0.39$. (c) The transverse component of the ion Coulomb force (red dashed line) and induced-dipole force (blue solid line) in trajectory (a). (d) same as (c) for trajectory (b). (e) Trajectories in the x-y plane corresponding to the trajectories in (a) (red dashed line) and (b) (blue solid line).

We now turn to the induced dipole force. Similar to the Coulomb interaction, the effect is strongest when the electron is near the ionic core: at birth and upon return. However, unlike the ionic Coulomb force, which is always attractive, the induced dipole force can be repulsive or attractive, depending on the direction of the laser field and the location of the electron. Figure 3 illustrates these effects for two typical trajectories: one at low energy (LES region) and a second at higher energy. The shaded regions in Figs. 3(a) and 3(b) indicate the time windows when the induced dipole force is repulsive (which means it pushes the electron away from $y = 0$) and in the nonshaded regions it is attractive. As shown in Fig. 3(c), the electron receives a repulsive kick at the beginning of the trajectory. Upon the first return, the induced dipole force again influences the trajectory, but the net effect is not significant because the direction of the force flips sign within a very short time window. Figure 3(d) shows a similar behavior for the trajectory with larger energy and so the net

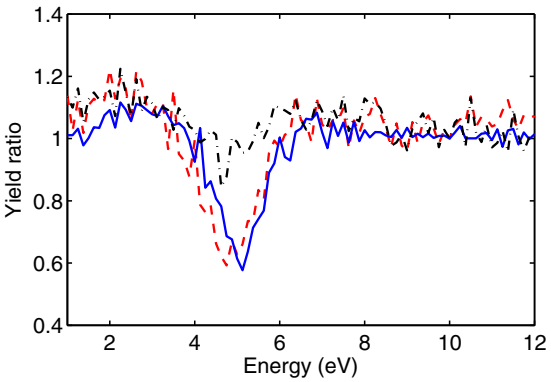

FIG. 4. Calculated yield ratios. Red dashed line: full simulation (same as Fig. 2). Blue solid line: same but induced dipole force turned on at $t = 5/4T$ until the end of the laser pulse. Black dashed-dotted line: induced dipole turned on only for $0 < t < T/4$. All three results are normalized at $E = 10$ eV. Parameters in the calculations: $I = 75$ TW/cm^2, $\lambda = 3$ μm; $\alpha = 79$ Å^3.

force at birth and first return is not critical for suppressing the LES. However, Fig. 3(c) shows that the repulsive kick at the second return ($t \sim 1.5T$) does result in a suppression since it opposes the Coulomb focusing (red solid line). Figure 3(e) shows the trajectories of Figs. 3(a) and 3(b) in the x-y plane, illustrated by the red dashed and blue lines, respectively. It shows that the low-energy trajectory (red dashed line) is suddenly deflected to a larger angle at the second return.

It is interesting to distinguish the induced dipole field effect at the second return from its effect at earlier times. This can be achieved by comparing simulations, in which the induced dipole force is turned on only within a specific time window, with full simulations. Thus, in Fig. 4, the blue solid line shows the yield ratio of a simulated spectrum with the induced dipole field starting at $t = 5T/4$ (i.e., the field influences the electron trajectories only during the second return and after) to the one without the induced dipole field; the red dashed line shows the ratio of a spectrum with the induced dipole field on at all times to the one without the induced dipole field; the black dashed-dotted line shows the ratio of a spectrum with the induced dipole field for $t \in [0, T/4]$ (i.e., the field influences the electron trajectories upon launching) to the one without the induced dipole field. The minimum at ∼5 eV (which indicates the suppression of the LES) in the blue solid line and the red dashed line are almost equal, thus confirming that the interaction at the second return is the origin of the suppression. On the other hand, the minimum in the black dashed-dotted line is much less pronounced, which implies that the repulsive force at the birth of the electron is not the main cause of the reduction. The simulations show that the reduction is caused by the influence of the induced dipole field on electron propagation.

IV. CONCLUSIONS

In conclusion, we have measured the low-energy structure in photoelectron distributions from C_{60} in the strong-field limit. Our study shows a significant reduction in the LES as compared to noble gases. Classical simulations reveal that the induced dipole field from the parent ion efficiently counteracts the bunching and focusing of the electron trajectories leading to a reduced LES. Simulations also reveal that its effect is concentrated around the second return of the electron to its parent ion. Thus, the LES might be a valuable spectroscopic feature that allows us to investigate the role of polarizability in strong-field processes.

ACKNOWLEDGMENTS

The work was supported by the National Science Foundation under Grant No. 1605042. The DiMauro Group acknowledges support of the Ohio Supercomputer Center (Project No. PAS0207). C.I.B. acknowledges support from the Air Force Office of Scientific Research Young Investigator Research Program (Award No. FA9550-15-1-0203). The Kling Group acknowledges support by the German Research Foundation via SPP1840 and the cluster of excellence "Munich Centre for Advanced Photonics." M.F.K. is grateful for support by the Max Planck Society.

[1] C. I. Blaga, F. Catoire, P. Colosimo, G. G. Paulus, H. G. Muller, P. Agostini, and L. F. DiMauro, Nat. Phys. **5**, 335 (2009).
[2] W. Quan, Z. Lin, M. Wu, H. Kang, H. Liu, X. Liu, J. Chen, J. Liu, X. He, S. Chen *et al.*, Phys. Rev. Lett. **103**, 093001 (2009).
[3] C. Liu and K. Z. Hatsagortsyan, Phys. Rev. Lett. **105**, 113003 (2010).
[4] T.-M. Yan, S. V. Popruzhenko, M. J. J. Vrakking, and D. Bauer, Phys. Rev. Lett. **105**, 253002 (2010).
[5] C. Lemell, K. I. Dimitriou, X.-M. Tong, S. Nagele, D. V. Kartashov, J. Burgdörfer, and S. Gräfe, Phys. Rev. A **85**, 011403 (2012).
[6] A. Kästner, U. Saalmann, and J. M. Rost, Phys. Rev. Lett. **108**, 033201 (2012).
[7] W. Becker, S. Goreslavski, D. Milošević, and G. Paulus, J. Phys. B **47**, 204022 (2014).
[8] D. Dimitrovski, J. Maurer, H. Stapelfeldt, and L. B. Madsen, Phys. Rev. Lett. **113**, 103005 (2014).
[9] F. Catoire, C. I. Blaga, E. Sistrunk, H. G. Muller, P. Agostini, and L. F. DiMauro, Laser Phys. **19**, 1574 (2009).
[10] C. Y. Wu, Y. D. Yang, Y. Q. Liu, Q. H. Gong, M. Y. Wu, X. Liu, X. L. Hao, W. D. Li, X. T. He, and J. Chen, Phys. Rev. Lett. **109**, 043001 (2012).
[11] M. G. Pullen, J. Dura, B. Wolter, M. Baudisch, M. Hemmer, N. Camus, A. Senftleben, C. D. Schroeter, R. Moshammer, J. Ullrich *et al.*, J. Phys. B **47**, 204010 (2014).
[12] M. Möller, F. Meyer, A. M. Sayler, G. G. Paulus, M. F. Kling, B. E. Schmidt, W. Becker, and D. B. Milošević, Phys. Rev. A **90**, 023412 (2014).
[13] B. Wolter, C. Lemell, M. Baudisch, M. G. Pullen, X.-M. Tong, M. Hemmer, A. Senftleben, C. D. Schröter, J. Ullrich, R. Moshammer *et al.*, Phys. Rev. A **90**, 063424 (2014).

[14] K. Zhang, Y. H. Lai, E. Diesen, B. E. Schmidt, C. I. Blaga, J. Xu, T. T. Gorman, F. Légaré, U. Saalmann, P. Agostini *et al.*, Phys. Rev. A **93**, 021403 (2016).
[15] V. R. Bhardwaj, P. B. Corkum, and D. M. Rayner, Phys. Rev. Lett. **91**, 203004 (2003).
[16] V. R. Bhardwaj, P. B. Corkum, and D. M. Rayner, Phys. Rev. Lett. **93**, 043001 (2004).
[17] S. Hunsche, T. Starczewski, A. l'Huillier, A. Persson, C.-G. Wahlström, H. B. van Linden van den Heuvell, and S. Svanberg, Phys. Rev. Lett. **77**, 1966 (1996).
[18] E. E. B. Campbell, K. Hansen, K. Hoffmann, G. Korn, M. Tchaplyguine, M. Wittmann, and I. V. Hertel, Phys. Rev. Lett. **84**, 2128 (2000).
[19] E. Campbell, K. Hoffmann, H. Rottke, and I. Hertel, J. Chem. Phys. **114**, 1716 (2001).
[20] M. Boyle, K. Hoffmann, C. P. Schulz, I. V. Hertel, R. D. Levine, and E. E. B. Campbell, Phys. Rev. Lett. **87**, 273401 (2001).
[21] D. Bauer, F. Ceccherini, A. Macchi, and F. Cornolti, Phys. Rev. A **64**, 063203 (2001).
[22] I. Shchatsinin, T. Laarmann, G. Stibenz, G. Steinmeyer, A. Stalmashonak, N. Zhavoronkov, C. P. Schulz, and I. V. Hertel, J. Chem. Phys. **125**, 194320 (2006).
[23] I. V. Hertel, I. Shchatsinin, T. Laarmann, N. Zhavoronkov, H.-H. Ritze, and C. P. Schulz, Phys. Rev. Lett. **102**, 023003 (2009).
[24] M. Kjellberg, O. Johansson, F. Jonsson, A. V. Bulgakov, C. Bordas, E. E. B. Campbell, and K. Hansen, Phys. Rev. A **81**, 023202 (2010).
[25] J. Johansson, J. Fedor, M. Goto, M. Kjellberg, J. Stenfalk, G. Henderson, E. Campbell, and K. Hansen, J. Chem. Phys. **136**, 164301 (2012).
[26] Y. Huismans, E. Cormier, C. Cauchy, P.-A. Hervieux, G. Gademann, A. Gijsbertsen, O. Ghafur, P. Johnsson, P. Logman, T. Barillot *et al.*, Phys. Rev. A **88**, 013201 (2013).
[27] H. Li, B. Mignolet, G. Wachter, S. Skruszewicz, S. Zherebtsov, F. Süßmann, A. Kessel, S. A. Trushin, N. G. Kling, M. Kübel, B. Ahn, D. Kim, I. Ben-Itzhak, C. L. Cocke, T. Fennel, J. Tiggesbäumker, K.-H. Meiwes-Broer, C. Lemell, J. Burgdörfer, R. D. Levine, F. Remacle, and M. F. Kling, Phys. Rev. Lett. **114**, 123004 (2015).
[28] H. Li, B. Mignolet, Z. Wang, K. Betsch, K. Carnes, I. Ben-Itzhak, C. Cocke, F. Remacle, and M. Kling, J. Phys. Chem. Lett. **7**, 4677 (2016).
[29] H. Xiong, B. Mignolet, L. Fang, T. Osipov, T. J. Wolf, E. Sistrunk, M. Gühr, F. Remacle, and N. Berrah, Sci. Rep. **7**, 121 (2017).
[30] I. V. Hertel, T. Laarmann, and C. P. Schulz, Adv. At. Mol. Opt. Phys. **50**, 219 (2005).
[31] F. Lépine, J. Phys. B **48**, 122002 (2015).
[32] H. Fuest, Y. H. Lai, C. I. Blaga, K. Suzuki, J. Xu, P. Rupp, H. Li, P. Wnuk, P. Agostini, K. Yamazaki, M. Kanno, H. Kono, M. F. Kling, and L. F. DiMauro, Phys. Rev. Lett. (to be published).
[33] M. Meckel, D. Comtois, D. Zeidler, A. Staudte, D. Pavičić, H. C. Bandulet, H. Pépin *et al.*, Science **320**, 1478 (2008).
[34] C. I. Blaga, J. Xu, A. D. DiChiara, E. Sistrunk, K. Zhang, Z. Chen, A.-T. Le *et al.*, Nature (London) **483**, 194 (2012).
[35] J. Xu, C. I. Blaga, K. Zhang, Y. H. Lai, C. D. Lin, T. A. Miller, P. Agostini, and L. F. DiMauro, Nat. Commun. **5**, 4635 (2014).
[36] K. J. Schafer, B. Yang, L. F. DiMauro, and K. C. Kulander, Phys. Rev. Lett. **70**, 1599 (1993).
[37] P. B. Corkum, Phys. Rev. Lett. **71**, 1994 (1993).
[38] A. Jaroń-Becker, A. Becker, and F. Faisal, J. Chem. Phys. **126**, 124310 (2007).
[39] M. Ruggenthaler, S. V. Popruzhenko, and D. Bauer, Phys. Rev. A **78**, 033413 (2008).
[40] F. Lépine and C. Bordas, Phys. Rev. A **69**, 053201 (2004).
[41] M. Ammosov, N. Delone, and V. Krainov, Sov. Phys. JETP **64**, 1191 (1986).
[42] N. I. Shvetsov-Shilovski, D. Dimitrovski, and L. B. Madsen, Phys. Rev. A **87**, 013427 (2013).